Lymphology 40 (2007) 63-73

CUTANEOUS DRAINAGE LYMPHATIC MAP WITH INTERSTITIAL MULTIDETECTOR-ROW COMPUTED TOMOGRAPHIC LYMPHOGRAPHY USING IOPAMIDOL: PRELIMINARY RESULTS

K. Suga, Y. Karino, T. Fujita, M. Okada, Y. Kawakami,K. Ueda, Y. Yuan, N. Matsunaga

Department of Radiology, Yamaguchi University School of Medicine, Yamaguchi, Japan

ABSTRACT

We performed preliminary tests of the feasibility of multi-detector computed tomographic lymphography (MDCT-LG) with interstitial injection of iopamidol for mapping cutaneous lymphatic drainage pathways. MDCT-LG images were obtained following cutaneous injection of a total of 1ml iopamidol bilaterally into hind legs of 10 dogs. The locations of the first draining lymph nodes were marked on the skin under MDCT-LG guidance. Five dogs served for postmortem examination of lymphatic anatomy, and the remaining 5 underwent MDCT-LG after ligation of the afferent lymphatic vessels of the first draining popliteal nodes. Clinically, MDCT-LG was attempted in 6 patients with cutaneous malignant melanoma and compared with Tc-99m-human serum albumin lymphoscintigraphy. MDCT-LG clearly visualized the first draining lymph nodes and their afferent lymphatic vessels draining from the contrast injection sites with detailed underlying anatomy in all dogs. At surgery, all these first draining nodes could be found at predicted locations under MDCT-LG guidance. MDCT-LG showed rerouting of lymphatic vessels after ligation of the afferent lymph vessels of the popliteal nodes in the second 5 dogs. Clinically, MDCT-LG also allowed accurate mapping and biopsy of the first draining nodes from primary tumors at predicted locations, with minimal skin incision. Lymphoscintigraphy failed to identify these nodes due to overlapping radioactivity of clustered nodes or transport of the radiotracer to subsequent distant nodes in 4 patients. Although a more extensive study is warranted for further validation, preoperative interstitial MDCT-LG appears to have the potential feasibility for accurate sentinel lymph node mapping and biopsy in patients with cutaneous melanoma.

Keywords: sentinel lymph node, cutaneous melanoma, computed tomography, lymphoscintigraphy, lymphography, iopamidol contrast agent

Surgical biopsy of the first draining lymph nodes (i.e., sentinel lymph node, SLNs) encountered from the lymphatic vessels directly draining the primary tumors is now emerging as a standard practice for accurate staging and prognostic prediction of the disease and for minimally invasive surgery in patients with cutaneous malignant melanoma (1-4). Currently, SLN mapping and biopsy in these patients are performed using a lymphoscintigraphic method with/without a combination of blue dye injection (3-13). However, these methods have certain limitations or disadvantages. The direct connection of primary SLNs and lymphatic vessels draining tumor sites, and accurate location, number and size of primary SLNs cannot be confirmed optimally due to limited spatial resolution of scintigrams (6,7,10).

Deeply lying SLNs in the neck may not be clearly delineated due to photon attenuation effect (6,8-10). Gamma probe survey often fails to detect SLNs close to the injection site of radiotracers because of shine-through radioactivity (7,10). Blue dye injection cannot clearly identify the lymphatic pathways to SLNs in fat-abundant tissues (7,9). There is a risk of labeling non-SLNs due to further migration of radiotracers or blue dye to subsequent distant nodes (9).

To resolve these problems with a lymphoscintigraphic method, we have recently developed multidetector-row computed tomographic lymphography (MDCT-LG) with interstitial injection of widely-available, water-soluble iodine contrast agent of iopamidol (14-18). This technique may be applicable for SLN mapping and biopsy in cutaneous malignant melanoma. In patients with breast cancer, this technique could accurately localize primary SLNs by clearly visualizing the direct connection of these nodes and their afferent lymphatic vessels draining from primary tumors and the underlying detailed anatomy, leading to favorable results with MDCT-LG-navigated SLN biopsy (18). The aim of the present study was to preliminarily test the feasibility of MDCT-LG for SLN mapping and biopsy in animals and patients with cutaneous malignant melanoma.

MATERIALS AND METHODS

Study Populations

Animal study

In accordance with the guidelines for the care and use of laboratory animals (19) and with approval by the institution's animal use and care administrative advisory committee, 10 female beagle dogs [10.7 ± 1.3 kg, mean ± standard deviation (SD)] kept without food for 4-6 hours preoperatively, were anesthetized with sodium pentobarbital (25 mg/kg, Dai-Nihon Pharmacy KK, Osaka, Japan), and ketamine hydrochloride (20 mg/kg, Bayer-Sankyo KK, Tokyo, Japan). The animals were placed in the supine position, intubated using a 7 mm cuffed endotracheal tube, and connected to a volume-cycled piston ventilator (Harvard Instrument Co., Cambridge Mass.) set at 15/min with a tidal volume of 15 ml/kg. Small supplementary doses of sodium pentobarbital (total dose ranging from 3.1 to 5.9 mg/kg) were administered intermittently as needed.

All animals underwent MDCT-LG after intra/subcutaneous injection of a total of 1 ml of widely available, extracellular contrast agent iopamidol (Iopamiron-370, Nippon Shering, Osaka, Japan) bilaterally into the target skin of the hind legs, as described below. Iopamiron-370 has a molecular weight of 777.09 Daltons, and the solute had an iodine concentration of 370 mg/ml, an osmolarity of 780 mOsm/kg, a viscosity of 9.1 mPa/sec, and pH of 6.5-7.5 (20). Five of these animals were euthanized for postmortem evaluation of lymphatic anatomy as described below. In the remaining 5 animals, MDCT-LG was repeated at 7 days after ligation of the efferent lymphatic vessels of the first draining popliteal nodes to evaluate the ability of MDCT-LG in depicting the rerouting of lymphatic pathways after lymphatic obstruction. The dog experiments were performed by three investigators (Ya. K., T.F. and KU) with over 5 years experience.

Clinical study

Interstitial MDCT-LG was performed in 6 patients with cutaneous malignant melanoma (age range: 54 to 78 years) with approval of the local ethics committee and informed consent (*Table 1*). These patients had primary cutaneous tumors with 1-4mm in thickness and no clinical evidence of any distant metastases at the time of diagnosis. All patients also underwent Technetium-99m-human serum albumin (Tc-99m-HSA) lymphoscintigraphy to compare with the results of MDCT-LG, as described below (21).

TABLE 1
Summary of the Results in 6 Patients with Cutaneous Malignant Melanoma

Patient No.	Age	Tumor location	Tumor size	SLN location	No. / Size of SLN identified on MDCT-LG	No. of SLN identified on Tc-99m-HSA lymphography	Histologic nodal status of SLN and non-SLN identified on MDCT-LG
1.	54/M	L foot	19 x 13 mm	L inguinal	2 / 4.6, 5.7 mm	2	SLN (2/2) = Negative non-SLN (6/6) = Negative
2.	70/M	R foot	24 x 14 mm	R inguinal	3 / 4.4, 5.3, 5.5 mm	3	SLN (3/3) = Negative non-SLN (5/5) = Negative
3.	74/F	L foot	22 x 11 mm	L inguinal	3 / 6.4, 8.1, 7.2 mm	5	SLN (3/3) = Negative non-SLN (8/8) = Negative
4.	63/F	R forearm	15 x 13 mm	R axillary	2 / 8.5, 6.2 mm	3	SLN (2/2) = Negative non-SLN (11/11) = Negative
5.	65/M	L forearm	22 x 17 mm	L axillary	3 / 5.1, 7.3, 8.4 mm	1	SLN (3/3) = Negative non-SLN (7/7) = Negative
6.	78/M	L forearm	14 x 12 mm	L axillary	2 / 6.8, 7.7 mm	4	SLN (2/2) = Negative non-SLN (8/8) = Negative

SLN = sentinel lymph node (the first drainage nodes), MDCT-LG = multi-detector computed tomographic lymphography,
Tc-99m-HSA = Technetium-99m-human serum albumin

Within 7 days after MDCT-LG, these patients underwent tumor resection and regional lymphadenectomy as described below.

MDCT-LG

Animal study

Interstitial MDCT-LG was performed using the MDCT scanner with a 0.5 mm x 4 detector rows (Siemens Volume Zoom, Siemens-Asahi Medical Ltd., Tokyo, Japan). In the animal study, each anesthetized animal was placed in the supine position on the CT table, and the lower legs were tightly and symmetrically fixed with cotton tapes. A total of 0.25 ml of 1% lidocaine hydrochloride was intra/subcutaneously injected into the target skin of the distal portion of the bilateral hind legs, using a 26-gauge, 5/8-inch hypodermic needle attached to a tuberculin syringe because a painless injection was favored in clinical setting. After local anesthesia, 1ml of iopamidol was injected intra/subcutaneously in the anesthetized skin area. The administration dose of iopamidol was determined according to our previous breast MDCT-LG study in dogs (15). The contrast injection sites were gently massaged for 30 seconds to facilitate migration of the contrast agent to draining lymphatic vessels (15). Contiguous 2 mm-thick transaxial CT images from the feet to inguinal regions were obtained prior to administration of the contrast agent and just after massage of the injection sites. CT scanning was operated at 120 kV, 100 mA, and a 32-cm field of view, 512 x 512 matrix, section spacing of 3 mm, and table speed of 1.53 mm/0.5 sec. The number of sections was individually adapted to ensure coverage of the regions of interest and ranged between 51 and 61, and the acquisition time ranged from 38 seconds to 46 seconds. Then, on the image viewer (Yokogawa-GE Medical, Tokyo, Japan) connected to CT scanner, multi-planar reconstruction (MPR) and three-dimensional (3D) surface- or volume-rendering maximum intensity projection (MIP) images were reconstructed from the 1.25 mm-thick post-contrast transaxial CT images. The location of the first draining nodes from the contrast injection sites was determined on MDCT-LG in consensus after independent interpretation by two radiologists (K. S., M.O.) with over 3 years experience regarding MDCT-LG evaluation of the breast region. The skin spots overlying these nodes were marked using a painting pen and a laser light navigation system equipped with the CT unit. The size and depth from the skin surface of these nodes were measured on transaxial MDCT-LG images. Enhancement of structures other than lymphatic pathways such as the venous system and muscles was also assessed by consensus of these observers.

In 5 of 10 dogs, MDCT-LG was repeated on 7 days after ligation of the efferent lymphatic vessels of the first draining popliteal nodes. In these animals, a total of 0.5 ml of 5% patent blue dye solution (Kanto Chemistry KK, Tokyo, Japan) was intra/subcutaneously injected into the same skin areas as in MDCT-LG to stain the lymphatic pathways. Under sterile conditions, a 3 cm incision was made in the popliteal region along the skin marker. After identifying the blue-staining popliteal nodes, their blue-staining afferent lymphatic vessels were ligated with a silk thread. The alteration of lymphatic pathways was assessed in consensus by the two radiologists (K. S., M.O.).

Clinical study

In patients with cutaneous melanoma, MDCT-LG was performed following local anesthesia with injection of a total dose of 0.25 ml of 1% lidocaine hydrochloride with a total intra/subcutaneous injection of 2-5 ml of iopamidol into 4 peritumoral areas. The dose of iopamidol was equally divided between these target areas. The administration dose of iopamidol was determined according to our previous MDCT-LG study in patients with breast cancer and was varied according to the

distance between the expected first draining nodes and the injection sites in individual patients. CT scanning covering the expected locations of the first draining nodes was performed prior to contrast injection and just after 30 seconds of massage at injection sites. CT scanning was operated at 100-120 kV, 20-260 mA, with a 45-cm field of view, 512 x 512 matrix, a section thickness of 3 mm and section spacing of 5 mm. The number of sections ranged between 36 and 40, with the acquisition time ranging from 22 sec to 25 sec. MPR and 3D MIP images were reconstructed from the 1.25 mm-thick post-contrast transaxial CT images on the image viewer. As in the animal study, the location of the first draining nodes was determined on MDCT-LG in consensus after independent interpretation by the two radiologists (K. S., M.O.), and the skin spots overlying these nodes were marked, and size and depth of these nodes measured. Enhancement of structures other than lymphatic pathways was also assessed by consensus of these observers. All the procedures including image processing were completed within 15 minutes for both animal and clinical studies.

All patients underwent Tc-99m-HSA lymphoscintigraphy 3 days before MDCT-LG. After local anesthesia, a total of 0.3 ml of 111MBq Tc-99m-HSA was intra/subcutaneously injected into 4 peritumoral areas as in MDCT-LG (21). Dynamic scintigrams were obtained with interval time of 30 seconds for 10 minutes after injection of the radiotracer. The hot spots of the first draining nodes were marked on the overlying skin under lymphoscintigraphy-guidance, by consensus of two radiologists (Ya.K, K.S) with over 5 years experience in lymphoscintigraphic evaluation. Thereafter, the location and number of these nodes on scintigrams were compared with those on MDCT-LG in each patient, by consensus of two experienced radiologists (K. S., M.O.).

Resection of the first draining nodes

The 5 animals were euthanized with intravenous injection of a 50 mg/kg of sodium pentobarbital for postmortem evaluation of lymphatic anatomy. Each animal was placed in the same position as in the CT study. The first draining nodes identified by MDCT-LG were searched and dissected under the guidance of the skin marker. The number, location and size of these nodes were compared with those on MDCT-LG by consensus of two observers (K. S. and Yu. K.).

For regional lymphadenectomy in patients, the surgeons searched the first draining nodes by referring to the anatomy of the lymphatic pathways on MDCT-LG, with a combined use of blue dye. A total of 5 ml of indigo carmine dye (Daiichi-seiyaku, Osaka, Japan) was cutaneously injected into the peritumoral areas. The surgeons took care to preserve the blue lymphatics intact until the first draining nodes were found under the skin markers and evaluated whether these nodes actually corresponded to the compatible position and size on the preoperative MDCT-LG. These first draining nodes and other distant nodes were resected and separately sent for histopathologic examination of the serial 1 mm-thick section specimens.

RESULTS

Animal Study

In all 10 dogs, cutaneous swelling at the injection sites was minor and quickly disappeared during MDCT-LG examination without any late adverse effects. MDCT-LG showed excellent opacification of the lymph nodes and lymphatic vessels draining from the contrast injection sites in all animals (*Figs. 1,2*). Among the draining lymphatic vessels, the superficial lateral and medial lymphatic vessels were most clearly visualized, although the deep medial vessels draining from the large popliteal nodes were visualized only in one leg of one dog. The oval shaped draining nodes with greater diameter than that of lymphatic vessels were

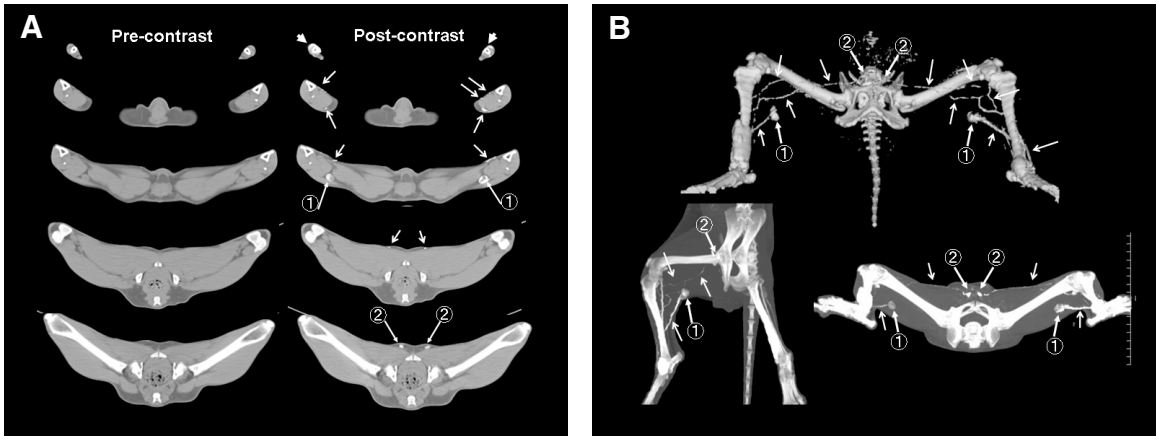

Fig. 1. Pre- and post-contrast transaxial images of MDCT-LG in a normal dog. (A) Transaxial MDCT-LG images obtained after 30 seconds massage of cutaneously injected sites of a 2 ml of iopamidol in dorsum of both hindpaws (arrow heads) visualize the draining lymphatic pathways of the hind legs, which are almost symmetric. The distal popliteal (①:→) and superficial inguinal (②:→) nodes are directly connected with the lymphatic vessels draining from the injection sites. (B) Multiple views of 3D surface- (top) and volume-rendering (bottom) MIP images reconstructed from transaxial MDCT-LG images provide the detailed anatomy of the lymphatic pathways and the location of the first draining distal popliteal (①:→) and superficial inguinal (②:→) nodes.

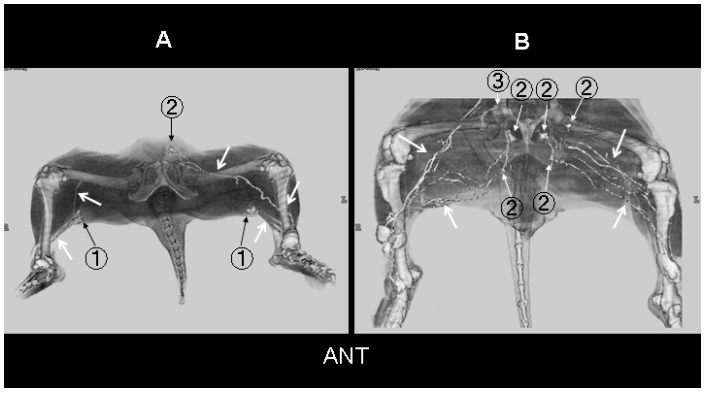

Fig. 2. 3D volume-rendering MIP images of MDCT-LG before (A) and after ligation (B) of the afferent lymphatic vessels of the first draining popliteal nodes in a dog. 3D MIP images before ligation of the bilateral afferent lymphatic vessels (A) visualize the distal popliteal (①:→) and superficial inguinal (②:→) nodes in the left limb and the distal popliteal nodes (①:→) in the right limb, with direct connection with their afferent lymphatic vessels draining from the contrast injection sites. After ligation of these afferent lymphatic vessels (B), the first draining popliteal nodes are not visualized. Instead, the lymphatic vessels (→) draining into the inguinal (②:→) or pelvic (③:→) nodes are visualized.

easily identified. MPR or 3D MIP MDCT-LG images facilitated the perception of the detailed anatomy of the complex lymphatic pathways. Overall, a total of 47 first draining nodes were identified, with a consistency between the two independent observers (*Figs. 1, 2*). These nodes were variably located in individual dogs (one distal popliteal node and one inguinal node in 12 legs of 7 dogs, one distal popliteal node and 2 inguinal nodes in 4 legs of 3 dogs, one distal and one proximal popliteal node and one inguinal

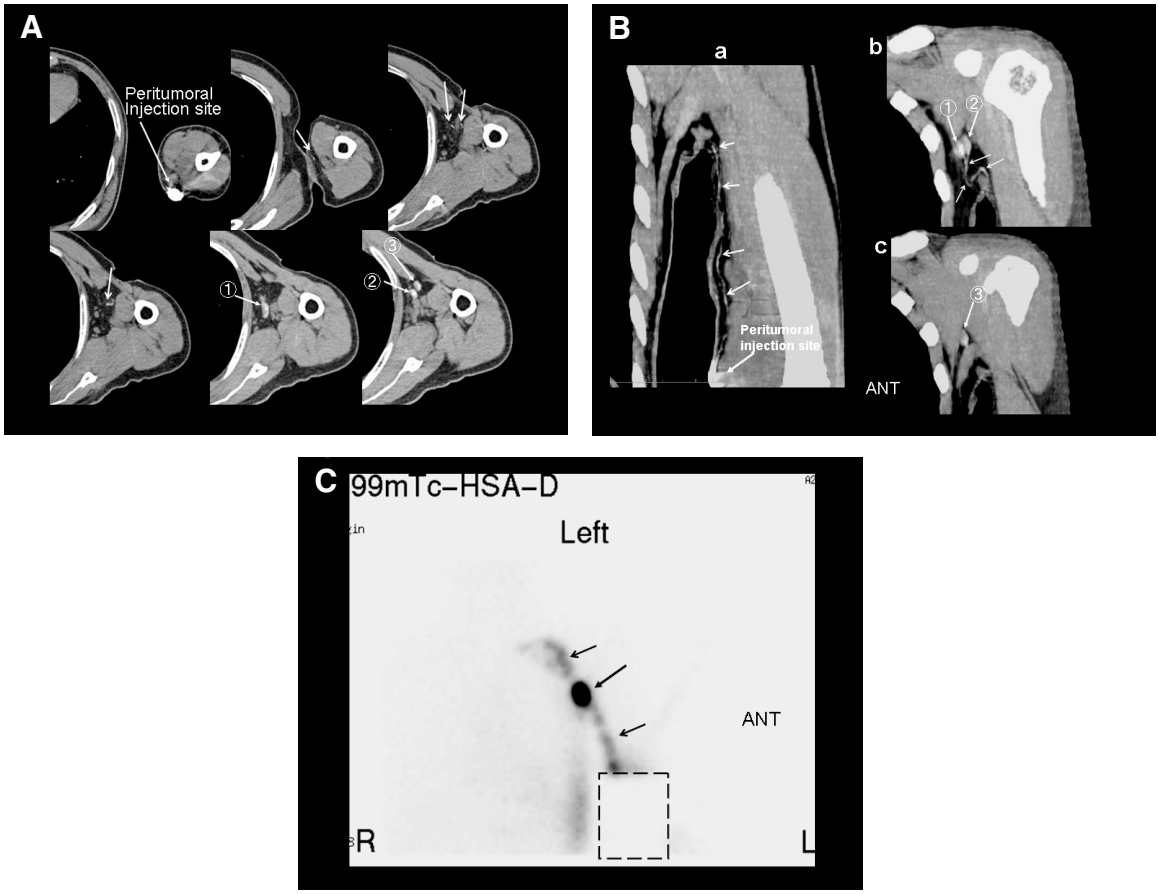

Fig. 3. Transaxial (A) and MPR (B) images of MDCT-LG, and Tc-99m-HSA lymphoscintigraphy (C) in a 65-year-old male with melanoma in the left forearm (Patient No. 5 in Table 1*). Transaxial MDCT-LG images (A) obtained after 30 seconds massage of the peritumoral injection sites of a total of 2 ml of iopamidol show the lymphatic vessels (→) draining into the three axillary nodes (①-③:→). MPR images (B; a-c) clearly visualized the anatomy of the draining lymphatic vessels (→) and those three first draining nodes (①-③:→). However, Tc-99m-HSA lymphoscintigraphy (C) shows only a single hot spot (→) connecting with its afferent and efferent lymphatic vessels (→), due to the overlapped radioactivity of the clustered first draining nodes. The dotted line square represents the shield for the injection site of the radiotracer.*

node in 2 legs of 2 dogs, one distal and one proximal popliteal nodes and 2 inguinal nodes in one leg of one dog, and one distal popliteal node alone in one leg of one dog). Among these nodes, the distal popliteal nodes had the larger size (average; 22.4 mm ± 1.7 in diameter, range: 18.4-25.3 mm) compared with remaining nodes (average; 4.2 mm ± 1.5, range; 3.4-7.2 mm). Avid opacification of these lymphatic pathways remained for sufficient time to mark the skin spots. No noticeable contrast enhancement was seen in the veins and muscles.

On post-mortem examination of the 5 dogs, all 23 first draining nodes identified by MDCT-LG could be accurately found and dissected at predicted locations under guidance of the skin markers. The size of these dissected nodes (average; 13.7 mm ± 9.8 in diameter, range; 4.0-25.3 mm) was consistent with that on the preoperative MDCT-LG (average; 13.4 mm ± 9.7, range; 3.7-24.7 mm).

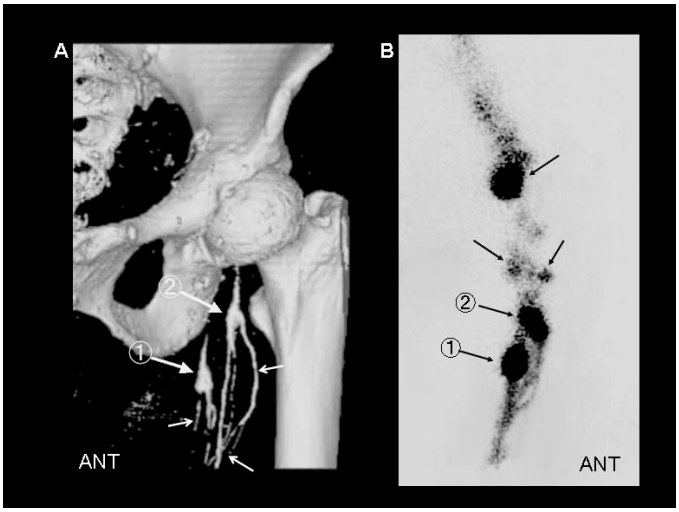

Fig. 4. Surface-rendering 3D MIP image of MDCT-LG (A), and Tc-99m-HSA lymphoscintigraphy (B) in a 54-year-old male with melanoma in the left foot (Patient No. 1 in Table 1). 3D MIP image (A) obtained with peritumoral injection of 5 ml of iopamidol clearly visualizes the direct connection of the two first lymph nodes (→) and lymphatic vessels (→) draining from the contrast injection sites. Tc-99m-HSA lymphoscintigraphy (B) shows two hot spots corresponding to those first draining nodes (→) connecting with their afferent and efferent lymphatic vessels (→), but also with other hot spots of the subsequent distant nodes. The detailed anatomy of these lymphatic pathways is obscure on the scintigram because of the limited spatial resolution.

In the remaining 5 dogs who underwent ligation of the afferent lymphatic vessels of the first draining distal popliteal nodes, focal soft tissue swelling was variably seen at the ligation sites. Although these nodes were not visualized on MDCT-LG after lymphatic ligation, other collateral lymphatic vessels draining into the inguinal or pelvic nodes were visualized (*Fig. 2*).

Clinical Study

As in the animal study, MDCT-LG clearly visualized the first nodes and their afferent lymphatic vessels draining from contrast injection sites in all 6 patients without any late adverse effects (*Figs. 3,4*). MPR and 3D MIP images also facilitated the visualization of the detailed anatomy of these lymphatic pathways (*Figs. 3,4*). Overall, a total of 15 first draining nodes (2.5 nodes per patient) were identified with consistency between the two independent observers *(Table 1*). Avid opacification of these lymphatic pathways remained for sufficient time to mark the skin spots overlying these nodes. Between MDCT-LG and Tc-99m-HSA lymphoscintigraphy, the location of these nodes appeared to be generally consistent in the patients studied. However, the number of these nodes was different in 4 (66%) patients due to overlapping radioactivity of clustered nodes or transport of the radiotracer to subsequent distant nodes (*Table 1*).

During operation, the routes of the blue lymphatic vessels appeared quite consistent with those identified on MDCT-LG, and the first draining nodes were accurately found and dissected at predicted locations under guidance of the skin markers in all patients. The size of these nodes (average; 6.5 mm ± 1.6, range; 4.6 -8.7 mm in diameter) was nearly consistent with those on MDCT-LG (average; 6.4 mm ± 1.3, range; 4.4-8.5 mm in diameter). In addition to these nodes, a total of 45 other distant nodes were dissected (*Table 1*). Histologically, no tumor metastases were found in any of these dissected nodes.

DISCUSSION

An essential prerequisite for a successful SLN biopsy procedure is accurate mapping of SLNs and their afferent lymphatic pathways draining from primary tumors (1-4). In the present study, interstitial MDCT-LG with iopamidol was able to accurately map the first draining nodes (i.e., SLNs), by visualizing the direct connection of these nodes and their afferent lymphatic vessels superimposed on the underlying detailed anatomy in dogs and patients with melanoma. This technique accurately identified the first draining nodes even when they were lying deeply, and their subsequent distant nodes were variably enhanced due to transport of iopamidol. The additional MIP and 3D MPR images facilitated the perception of the complex lymphatic pathways. At surgery, all the first draining nodes preoperatively identified by this technique could be correctly found or dissected at the predicted locations under guidance of skin markers. Although further validation is required in more extensive animal and clinical studies, these preliminary results indicate the potential feasibility of interstitial MDCT-LG for SLN mapping and biopsy in cutaneous malignant melanoma.

SLN mapping and biopsy in cutaneous melanoma are currently performed using radiocolloid lymphoscintigraphy and intraoperative gamma probe with/without a combined use of blue dye (6,9-13). However, these methods have certain disadvantages in accurate SLN mapping and biopsy (4,9,15-22). Lymphoscintigraphy cannot precisely predict accurate location and number of SLNs due to the limitation of spatial resolution of scintigrams, overlapped radioactivity of clustered SLNs and transport of radiotracers from primary SLNs to the subsequent distant nodes (7-11,14). Gamma probe survey has difficulty in detection of SLN close to the injection site because of “shine-through” radioactivity (7,10). There is no definitive criteria for defining SLN in regard to the level of radioactivity and blue staining (7,9,10). Deeper lying blue lymphatic vessels and lymph nodes are not easily found during operation (10). The ability of the present MDCT-LG to directly visualize the first nodes and their afferent lymphatic vessels draining from contrast injection sites with anatomic details avoids these disadvantages of scintigraphic and blue dye methods. This technique also is safe and can be quickly performed at any time before surgery (14-18).

The lymphatic pathways visualized on MDCT-LG in our dogs closely approximates the descriptions in the anatomic text of dogs (22). However, the efferent lymphatic vessels from the large distal popliteal nodes were infrequently visualized on MDCT-LG in our study. This may be caused by slow transit and sequestration of iopamidol in the sinusoids of these nodes. The lymphatic pathways in the right and left legs were also occasionally asymmetric on MDCT-LG. This feature may be caused by asymmetric lymphatic drainage from the contrast injection sites at different locations.

The increase in lymphatic vessels and alteration of the draining nodes on MDCT-LG in our dogs who underwent lymphatic ligation are consistent with the previous lymphoscintigraphic findings in patients with lymphatic obstruction (23,24). The increased lymphatic vessels represent collateral lymphatic flow or neovascularization associated with lymphatic obstruction (24). The alteration in the draining nodes is caused by the recruiting of lymphatic drainage after lymphatic obstruction (16). These findings may explain the complications (focal lymphedema and late nodal metastases) associated with SLN biopsy or tumor resection (25-28). MDCT-LG after these surgical interventions will also be useful in clarifying the causes of these complications.

Iopamidol is considered to drain mainly from the interstitial space to lymphatic pathways through the thin-walled and fenestrated lymphatic microvessels (14-15,29,30). The avid opacification of the first draining nodes

may be related to slow transit and sequestration of iopamidol in the nodal sinusoid. The present procedure of multiple peritumoral injections of iopamidol should facilitate visualization of draining lymphatic pathways (3,7,9,11). The negligible enhancement of the venous system is advantageous for obtaining a good quality MDCT-LG, although iopamidol may partly drain to this system. However, the range of visualized draining lymphatic pathways should vary according to injection sites and administration dose of iopamidol, as well as timing of CT scanning. Although the present MDCT-LG obtained at an early time after injection of the relatively low dose of iopamidol was able to visualize the main stream of lymph flow and the first draining nodes in our patients, further study is warranted to optimize the MDCT-LG procedure for primary tumors at various locations.

In conclusion, our preliminary results indicate the potential feasibility of interstitial MDCT-LG with iopamidol for accurate SLN mapping and biopsy in cutaneous melanoma. This study sets up the framework for more extensive animal and clinical studies for further validation of this technique.

ACKNOWLEDGMENTS

This study was supported in part by the Grant for Scientific Research (16591206) from the Japanese Ministry of Education, Science, Sports & Culture.

REFERENCES

1. Cabanas, RM: An approach for the treatment of penile carcinoma. Cancer 39 (1977), 456.
2. Cabanas, RM: The concept of the sentinel lymph node. Recent Results. Cancer Res. 157 (2000), 109.
3. Uren, RF, R Howman-Giles, JF Thompson, et al: The impact of lymphoscintigraphy technique on the outcome of sentinel node biopsy in 1,313 patients with cutaneous melanoma: An Italian multicentric study (SOLISM-IMI). J. Nucl. Med. 47 (2006), 234.
4. Leong, SP: The role of sentinel lymph nodes in malignant melanoma. Surg. Clin. North. Am. 80 (2000), 1741.
5. Morton, DL, JF Thompson, R Essner, et al: Validation of the accuracy of intraoperative lymphatic mapping and sentinel lymphadenectomy for early-stage melanoma: A multicenter trial. Multicenter Selective Lymphadenectomy Trial Group. Ann. Surg. 230 (1999), 453.
6. Lee, KK, JT Vetto, K Mehrany, et al: Sentinel lymph node biopsy. Clin. Dermatol. 22 (2004), 234.
7. Mariani, G, M Gipponi, L Moresco, et al. Radioguided sentinel node biopsy in malignant cutaneous melanoma. J. Nucl. Med. 43 (2002), 811.
8. Gershenwald, JE, W Thompson, PF Mansfield, et al: Multi-institutional melanoma lymphatic mapping experience: The prognostic value of sentinel lymph node status in 612 stage 1 or 2 melanoma patients. J. Clin. Oncol. 17 (1999), 976.
9. Cochran, AJ, A Roberts, DR Wennb, et al: Update on lymphatic mapping and sentinel node biopsy in the management of patients with melanocytic tumours. Pathology 36 (2004),478.
10. Stadelmann, WK, L Cobbins, EJ Lentsch: Incidence of nonlocalization of sentinel lymph nodes using preoperative lymphoscintigraphy in 74 consecutive head and neck melanoma and Merkel cell carcinoma patients. Ann. Plast. Surg. 52 (2004), 546.
11. Leong, SP, EF Morita, M Sudmeyer, et al: Heterogeneous patterns of lymphatic drainage to sentinel lymph nodes by primary melanoma from different anatomic sites. Clin. Nucl. Med. 30 (2005), 150.
12. Menes, TS, J Schachhter, AP Steinmetz, et al: Lymphatic drainage to the popliteal basin in distal lower extremity malignant melanoma. Arch. Surg. 139 (2004), 1002.
13. Picciotto, F, A Zaccagna, G Derosa, et al: Clear cell sarcoma (malignant melanoma of soft parts) and sentinel lymph node biopsy. Eur. J. Dermatol. 15 (2005), 46.
14. Suga, K, N Ogasawara, M Okada, et al: Interstitial CT lymphography-guided localization of breast sentinel lymph node: Preliminary results. Surgery 133 (2003), 170.
15. Suga, K, N Ogasawara, Y Yuan, et al: Visualization of breast lymphatic pathways with an indirect CT lymphography using a nonionic monometric contrast medium iopamidol: Preliminary results. Invest. Radiol. 38 (2003), 73-84.
16. Suga, K, Y Yuan, M Okada, et al: Breast sentinel lymph node mapping at CT

lymphography with iopamidol. Preliminary experience. Radiology 230 (2003), 543.
17. Tangoku, A, S Yamamoto, K Suga, et al: Sentinel lymph node biopsy using computed tomography–lymphography in patients with breast cancer. Surgery 135 (2004), 258.
18. Suga, K, S Yamamoto, A Tangoku, et al: Breast sentinel lymph node navigation with three-dimensional interstitial multidetector-row computed tomographic lymphography. Invest. Radiol. 40(2005), 336.
19. National Research Council. *Guide for the Care and Use of Laboratory Animals*. 7th ed. Washington, DC, National Academy Press, 1996.
20. Spatro, RF: New and old contrast agents: Pharmacology, tissue opacification, and excretory urography. Urol. Radiol. 10 (1988), 2.
21. Suga, K, Kume N, Matsunaga N, et al: Assessment of leg oedema by dynamic lymphoscintigraphy with intradermal injection of Tc-99m-human serum albumin and load produced by standing. Eur. J. Nucl. Med. 28 (2001), 294.
22. Evans, C: The lymphatic system. In: *Miller's Anatomy of the Dog*. 2nd ed. Philadelphia: Saunders, 1979, 834-835.
23. Intezo, CM, SM Kim, JI Patel, et al: Lymphoscintigraphy in cutaneous melanoma: a total body atlas of sentinel node mapping. Radiographics 22 (2002), 491.
24. Burnand, KG, CL McGuinness, NR Lagattolla, et al: Value of isotope lymphography in the diagnosis of lymphedema of the leg. Br. J. Surg. 89 (2002),74.
25. Roaten, JB, N Pearman, R Gonzalez, et al: Identifying risk factors for complications following sentinel lymph node biopsy for melanoma. Arch. Surg. 140 (2005), 85.
26. Wasserberg, N, H Tulchinsky, J Schchter, et al: Sentinel-lymph-node (SLNB) for melanoma is not complication-free. Eur. J. Surg. Oncol. 30 (2004), 851.
27. Wrone, DA, KK Tanabe, AB Cosimi, et al: Lymphedema after sentinel lymph node biopsy for cutaneous melanoma. Arch. Dermatol. 136 (2000), 511.
28. Vries, M de, WG Vonkeman, RJ van Ginkel, et al: Morbidity after axillary sentinel lymph node biopsy in patients with cutaneous melanoma. Eur. J. Surg. Oncol. 23 (2005), 4312.
29. Lubach, D, W Ludemann, V Berens, et al: Recent findings on the angio-architecture of the lymph vessel system of human skin. Br. J. Dermatol. 135 (1996), 733.
30. Schmid-Schonbein, GW: Microlymphatics and lymph flow. Physiol. Rev. 70 (1990), 987.

Kazuyoshi Suga, MD
Department of Radiology
Yamaguchi University School of Medicine
1-1-1 Minami-Kogushi, Ube
Yamaguchi 755-8505, Japan
TEL: +81-836-51-5111
FAX: +81-836-51-9999
E-mail: sugar@po.cc.yamaguchi-u.ac.jp